hp-Version Trefftz Discontinuous Galerkin Method for the Homogeneous Helmholtz Equation

Scott Congreve

Fakultät für Mathematik, Universität Wien

Joint work with
Ilaria Perugia (Universität Wien)
Paul Houston (University of Nottingham)

Workshop on CENTRAL Trends in PDEs

Let $\Omega \subset \mathbb{R}^d$, $d = 2, 3$ be a bounded polygonal/polyhedral domain.

$$\begin{aligned} -\Delta u - k^2 u &= 0 && \text{in } \Omega, \\ u &= 0 && \text{on } \Gamma_D, && \text{(sound-soft scattering)} \\ \nabla u \cdot \boldsymbol{n} &= 0 && \text{on } \Gamma_N, && \text{(sound-hard scattering)} \\ \nabla u \cdot \boldsymbol{n} + ik\vartheta u &= g_R && \text{on } \Gamma_R. \end{aligned}$$

Let $\Omega \subset \mathbb{R}^d$, $d = 2, 3$ be a bounded polygonal/polyhedral domain.

$$\begin{aligned} -\Delta u - k^2 u &= 0 && \text{in } \Omega, \\ u &= 0 && \text{on } \Gamma_D, && \text{(sound-soft scattering)} \\ \nabla u \cdot \boldsymbol{n} &= 0 && \text{on } \Gamma_N, && \text{(sound-hard scattering)} \\ \nabla u \cdot \boldsymbol{n} + ik\vartheta u &= g_R && \text{on } \Gamma_R. \end{aligned}$$

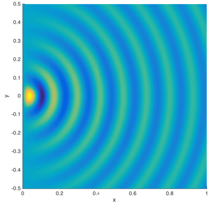

Acoustic Wave Prop.

Let $\Omega \subset \mathbb{R}^d$, $d = 2, 3$ be a bounded polygonal/polyhedral domain.

$$\begin{aligned} -\Delta u - k^2 u &= 0 && \text{in } \Omega, \\ u &= 0 && \text{on } \Gamma_D, && \text{(sound-soft scattering)} \\ \nabla u \cdot \boldsymbol{n} &= 0 && \text{on } \Gamma_N, && \text{(sound-hard scattering)} \\ \nabla u \cdot \boldsymbol{n} + ik\vartheta u &= g_R && \text{on } \Gamma_R. \end{aligned}$$

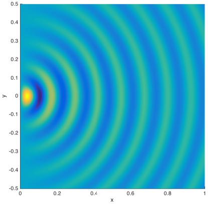

Acoustic Wave Prop.

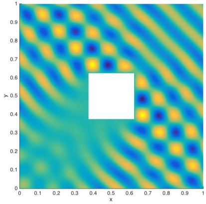

Sound-soft Scattering

Helmholtz Equation

Let $\Omega \subset \mathbb{R}^d$, $d = 2, 3$ be a bounded polygonal/polyhedral domain.

$$
\begin{aligned}
-\Delta u - k^2 u &= 0 && \text{in } \Omega, && \\
u &= 0 && \text{on } \Gamma_D, && \text{(sound-soft scattering)} \\
\nabla u \cdot \boldsymbol{n} &= 0 && \text{on } \Gamma_N, && \text{(sound-hard scattering)} \\
\nabla u \cdot \boldsymbol{n} + ik\vartheta u &= g_R && \text{on } \Gamma_R. &&
\end{aligned}
$$

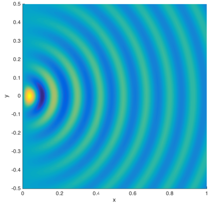

Acoustic Wave Prop.

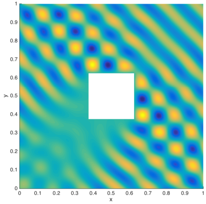

Sound-soft Scattering

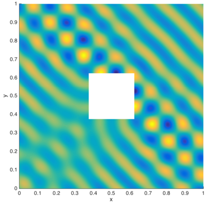

Sound-hard Scattering

Problems with FEM:

- Number of *degrees of freedom* required to obtain given accuracy increases with wave number k.
- h-version FEM affected by pollution effect [Babuška & Sauter, 2000]:

$$\|u - u_h\| \leq C(k) \inf_{v_h \in V(\mathcal{T}_h)} \|u - v_h\|$$

$C(k)$ is an increasing function in k.

Problems with FEM:

- Number of *degrees of freedom* required to obtain given accuracy increases with wave number k.
- h-version FEM affected by pollution effect [Babuška & Sauter, 2000]:

$$\|u - u_h\| \leq C(k) \inf_{v_h \in V(\mathcal{T}_h)} \|u - v_h\|$$

$C(k)$ is an increasing function in k.

We incorporate information about the frequency into the finite element space to attempt to reduce computation cost.

Polynomial DG Finite Element Spaces: DGFEM uses polynomial basis functions defined on a reference element $\widehat{K}$:

$$V_q^{DG}(\mathcal{T}_h) := \{v \in L^2(\Omega) : v|_K \circ F_K \in \mathcal{S}_{q_K}(\widehat{K}), K \in \mathcal{T}_h\}.$$

Trefftz FEM Spaces

Polynomial DG Finite Element Spaces: DGFEM uses polynomial basis functions defined on a reference element $\widehat{K}$:

$$V_q^{DG}(\mathcal{T}_h) := \{v \in L^2(\Omega) : v|_K \circ F_K \in \mathcal{S}_{q_K}(\widehat{K}), K \in \mathcal{T}_h\}.$$

Trefftz Finite Element Space: Use basis functions defined element-wise based on general solutions to the PDE.
First define the local Trefftz spaces

$$T(K) := \{v|_K : -\Delta u - k^2 u = 0\}$$

and let

$$T(\mathcal{T}_h) := \{v \in L^2(\Omega) : v|_K \in T(K), K \in \mathcal{T}_h\}.$$

Polynomial DG Finite Element Spaces: DGFEM uses polynomial basis functions defined on a reference element $\widehat{K}$:

$$V_q^{DG}(\mathcal{T}_h) := \{v \in L^2(\Omega) : v|_K \circ F_K \in \mathcal{S}_{q_K}(\widehat{K}), K \in \mathcal{T}_h\}.$$

Trefftz Finite Element Space: Use basis functions defined element-wise based on general solutions to the PDE.
First define the local Trefftz spaces

$$T(K) := \{v|_K : -\Delta u - k^2 u = 0\}$$

and let

$$T(\mathcal{T}_h) := \{v \in L^2(\Omega) : v|_K \in T(K), K \in \mathcal{T}_h\}.$$

We let $V_p(K) \subset T(K)$ be a finite dimensional local space; then, the Trefftz FE Space is given by

$$V_p(\mathcal{T}_h) := \{v \in T(\mathcal{T}_h) : v_K \in V_p(K), K \in \mathcal{T}_h\}.$$

For Helmholtz we can use the following basis functions:

Plane Waves: $\boldsymbol{x} \mapsto \mathrm{e}^{ik\boldsymbol{d}\cdot\boldsymbol{x}}$, where $\boldsymbol{d}$ is a direction vector.

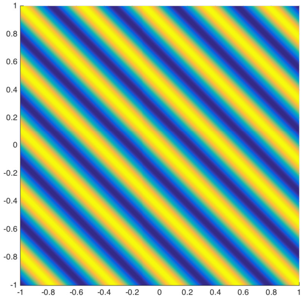

For Helmholtz we can use the following basis functions:

Plane Waves: $\boldsymbol{x} \mapsto \mathrm{e}^{ik\boldsymbol{d}\cdot\boldsymbol{x}}$, where $\boldsymbol{d}$ is a direction vector.

Circular/Spherical Waves $\boldsymbol{x} \mapsto \mathcal{J}_\ell(k|\boldsymbol{x}|)\mathrm{e}^{i\ell\theta}$ (in 2D), where θ is the angle of $\boldsymbol{x}$ in polar coordinates, $\ell \in \mathbb{Z}$, and $\mathcal{J}_\ell$ is the Bessel function of the first kind of order ℓ.

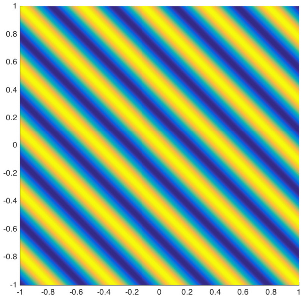

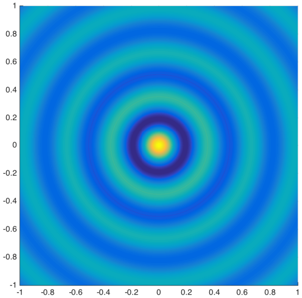

Plane Waves

$$V_p(K) = \left\{ v : v(\boldsymbol{x}) = \sum_{\ell=1}^{p_K} \alpha_\ell \mathrm{e}^{ik\boldsymbol{d}_\ell \cdot (\boldsymbol{x} - \boldsymbol{x}_k)}, \alpha_\ell \in \mathbb{C} \right\}$$

where p_K is the number of *degrees of freedom* for the element K, $\boldsymbol{d}_l$, $l = 1, \cdots, N_K$ are p_K (roughly) evenly spaced unit direction vectors, and $\boldsymbol{x}_K$ is the centre of the element.

$$V_p(K) = \left\{ v : v(\boldsymbol{x}) = \sum_{\ell=1}^{p_K} \alpha_\ell \mathrm{e}^{ik\boldsymbol{d}_\ell \cdot (\boldsymbol{x} - \boldsymbol{x}_k)}, \alpha_\ell \in \mathbb{C} \right\}$$

where p_K is the number of *degrees of freedom* for the element K, $\boldsymbol{d}_l$, $l = 1, \cdots, N_K$ are p_K (roughly) evenly spaced unit direction vectors, and $\boldsymbol{x}_K$ is the centre of the element.

Trefftz DG has less degrees of freedom than high-order polynomials for the same accuracy.

Basis Functions	2D	3D
DG ($\mathcal{P}_q$)	$(q+1)(q+2)/2$	$(q+1)(q+2)(q+3)/6$
DG ($\mathcal{Q}_q$)	$(q+1)^2$	$(q+1)^3$
Trefftz DG	$2q+1$	$(q+1)^2$

Number of Degrees of Freedom

Plane Waves

$$V_p(K) = \left\{ v : v(\boldsymbol{x}) = \sum_{\ell=1}^{p_K} \alpha_\ell \mathrm{e}^{ik\boldsymbol{d}_\ell \cdot (\boldsymbol{x} - \boldsymbol{x}_k)}, \alpha_\ell \in \mathbb{C} \right\}$$

where p_K is the number of *degrees of freedom* for the element K, $\boldsymbol{d}_l$, $l = 1, \cdots, N_K$ are p_K (roughly) evenly spaced unit direction vectors, and $\boldsymbol{x}_K$ is the centre of the element.

Trefftz DG has less degrees of freedom than high-order polynomials for the same accuracy.

Basis Functions	2D	3D
DG ($\mathcal{P}_q$)	$(q+1)(q+2)/2$	$(q+1)(q+2)(q+3)/6$
DG ($\mathcal{Q}_q$)	$(q+1)^2$	$(q+1)^3$
Trefftz DG	$2q+1$	$(q+1)^2$

Number of Degrees of Freedom

Direction Vectors ($q = 3$):

2D

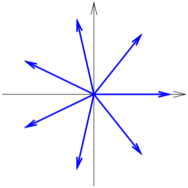

3D

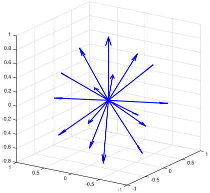

[Sloan & Womersley, 2004]

TDG/DG FEM Comparison

Consider the smooth (analytic) solution (for Acoustic Wave Propagation)

$$u(r,\theta) = \mathcal{J}_1(kr)\cos(\theta)$$

for $k = 20$ on the domain $\Omega = (0,1) \times (-1/2, 1/2)$.

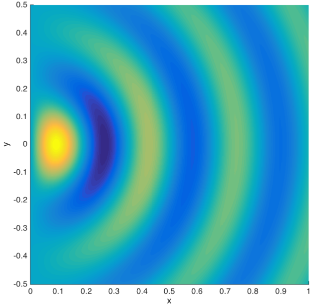

Analytical Solution
(Real Part)

Consider the smooth (analytic) solution (for Acoustic Wave Propagation)

$$u(r,\theta) = \mathcal{J}_1(kr)\cos(\theta)$$

for $k = 20$ on the domain $\Omega = (0,1) \times (-1/2, 1/2)$.
We solve using both a DGFEM (solid line) and Trefftz DGFEM (dashed).

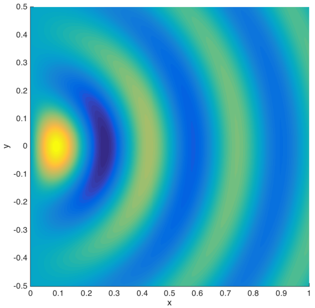

Analytical Solution
(Real Part)

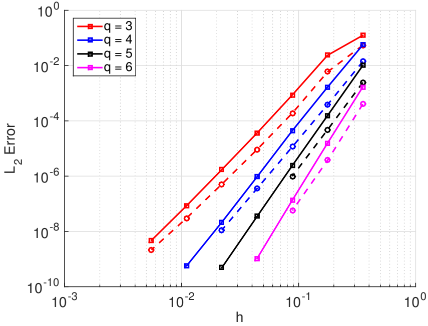

$\|u - u_{hp}\|_{L^2(\Omega)}$ vs. h
(h-refinement)

TDG/DG FEM Comparison

Consider the smooth (analytic) solution (for Acoustic Wave Propagation)

$$u(r,\theta) = \mathcal{J}_1(kr)\cos(\theta)$$

for $k = 20$ on the domain $\Omega = (0,1) \times (-1/2, 1/2)$.
We solve using both a DGFEM (solid line) and Trefftz DGFEM (dashed).

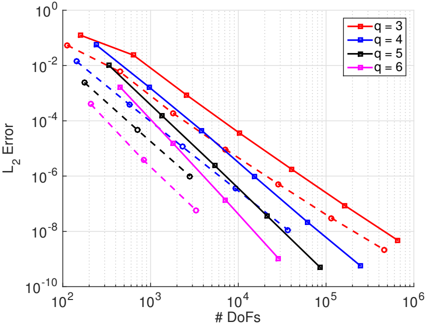

$\|u - u_{hp}\|_{L^2(\Omega)}$ vs. Degrees of Freedom
(h-refinement)

TDG/DG FEM Comparison

universität wien

Consider the smooth (analytic) solution (for Acoustic Wave Propagation)

$$u(r,\theta) = \mathcal{J}_1(kr)\cos(\theta)$$

for $k = 20$ on the domain $\Omega = (0,1) \times (-1/2, 1/2)$.
We solve using both a DGFEM (solid line) and Trefftz DGFEM (dashed).

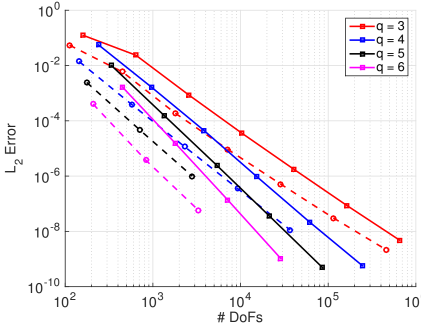

$\|u - u_{hp}\|_{L^2(\Omega)}$ vs. Degrees of Freedom (h-refinement)

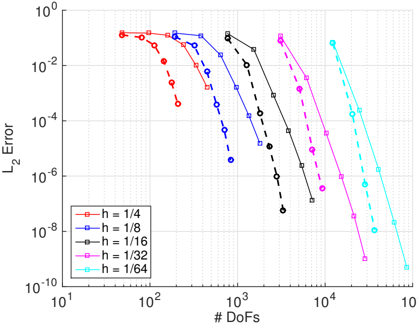

$\|u - u_{hp}\|_{L^2(\Omega)}$ vs. Degrees of Freedom (p-refinement)

TDGFEM for Helmholtz

Given a mesh $\mathcal{T}_h$ on Ω we derive the TDGFEM as follows.

Given a mesh $\mathcal{T}_h$ on Ω we derive the TDGFEM as follows.

- Multiply by test functions and integrate by parts, element-wise, twice (ultra weak formulation):

$$\int_K (-\Delta u - k^2 u)\,\bar{v} \quad d\boldsymbol{x} = 0$$

universität wien

Given a mesh $\mathcal{T}_h$ on Ω we derive the TDGFEM as follows.

- Multiply by test functions and integrate by parts, element-wise, twice (ultra weak formulation):

$$\int_K (\nabla u \cdot \nabla \bar{v} - k^2 u \bar{v}) \, d\boldsymbol{x} \qquad - \int_{\partial K} \nabla u \cdot \boldsymbol{n}_K \bar{v} \, ds = 0$$

Given a mesh $\mathcal{T}_h$ on Ω we derive the TDGFEM as follows.

- Multiply by test functions and integrate by parts, element-wise, twice (ultra weak formulation):

$$\int_K u(-\Delta \bar{v} - k^2 \bar{v}) \; d\boldsymbol{x} + \int_{\partial K} u \nabla \bar{v} \cdot \boldsymbol{n}_K \, ds - \int_{\partial K} \nabla u \cdot \boldsymbol{n}_K \bar{v} \, ds = 0$$

Given a mesh $\mathcal{T}_h$ on Ω we derive the TDGFEM as follows.

- Multiply by test functions and integrate by parts, element-wise, twice (ultra weak formulation):

$$\int_K u(-\Delta \bar{v} - k^2 \bar{v}) \quad d\boldsymbol{x} + \int_{\partial K} u \nabla \bar{v} \cdot \boldsymbol{n}_K \, ds - \int_{\partial K} \nabla u \cdot \boldsymbol{n}_K \bar{v} \, ds = 0$$

TDGFEM for Helmholtz

Given a mesh $\mathcal{T}_h$ on Ω we derive the TDGFEM as follows.

- Multiply by test functions and integrate by parts, element-wise, twice (ultra weak formulation):

$$\int_K u(-\Delta \bar{v} - k^2 \bar{v}) \quad d\boldsymbol{x} + \int_{\partial K} u \nabla \bar{v} \cdot \boldsymbol{n}_K \, ds - \int_{\partial K} \nabla u \cdot \boldsymbol{n}_K \bar{v} \, ds = 0$$

TDGFEM for Helmholtz

Given a mesh $\mathcal{T}_h$ on Ω we derive the TDGFEM as follows.

- Multiply by test functions and integrate by parts, element-wise, twice (ultra weak formulation):

$$\int_K u(-\Delta \bar{v} - k^2 \bar{v}) \, d\boldsymbol{x} + \int_{\partial K} u \nabla \bar{v} \cdot \boldsymbol{n}_K \, ds - \int_{\partial K} \nabla u \cdot \boldsymbol{n}_K \bar{v} \, ds = 0$$

- Replace continuous functions by discrete approximations ($u_{hp}, v_{hp} \in V_p(\mathcal{T}_h)$) and traces by numerical fluxes

$$u \to \widehat{u}_{hp}, \qquad \nabla u \to ik\widehat{\boldsymbol{\sigma}}_{hp}.$$

Given a mesh $\mathcal{T}_h$ on Ω we derive the TDGFEM as follows.

- Multiply by test functions and integrate by parts, element-wise, twice (ultra weak formulation):

$$\int_K u(-\Delta\bar{v} - k^2\bar{v}) \;\; d\boldsymbol{x} + \int_{\partial K} u\nabla\bar{v}\cdot\boldsymbol{n}_K\, ds - \int_{\partial K} \nabla u\cdot\boldsymbol{n}_K\bar{v}\, ds = 0$$

- Replace continuous functions by discrete approximations ($u_{hp}, v_{hp} \in V_p(\mathcal{T}_h)$) and traces by numerical fluxes

$$u \to \widehat{u}_{hp}, \qquad \nabla u \to ik\widehat{\boldsymbol{\sigma}}_{hp}.$$

- $v \in V_p(\mathcal{T}_h) \subset T(\mathcal{T}_h) \quad \Longrightarrow \quad -\Delta\bar{v} - k^2\bar{v} = 0$ in K.

TDGFEM for Helmholtz

Given a mesh $\mathcal{T}_h$ on Ω we derive the TDGFEM as follows.

- Multiply by test functions and integrate by parts, element-wise, twice (ultra weak formulation):

$$\int_K u(-\Delta \bar{v} - k^2 \bar{v}) \;\; d\boldsymbol{x} + \int_{\partial K} u \nabla \bar{v} \cdot \boldsymbol{n}_K \, ds - \int_{\partial K} \nabla u \cdot \boldsymbol{n}_K \bar{v} \, ds = 0$$

- Replace continuous functions by discrete approximations $(u_{hp}, v_{hp} \in V_p(\mathcal{T}_h))$ and traces by numerical fluxes

$$u \to \widehat{u}_{hp}, \qquad \nabla u \to ik\widehat{\boldsymbol{\sigma}}_{hp}.$$

- $v \in V_p(\mathcal{T}_h) \subset T(\mathcal{T}_h) \quad \Longrightarrow \quad -\Delta \bar{v} - k^2 \bar{v} = 0 \text{ in } K.$

$$\int_{\partial K} \widehat{u}_{hp} \nabla \bar{v}_{hp} \cdot \boldsymbol{n}_K \, ds - \int_{\partial K} ik\widehat{\boldsymbol{\sigma}}_{hp} \cdot \boldsymbol{n}_K \bar{v}_{hp} \, ds = 0, \qquad \text{for all } K \in \mathcal{T}_h.$$

$$\{\!\{v\}\!\} = \frac{v^+ + v^-}{2}, \quad [\![v]\!] = v^+\boldsymbol{n}^+ + v^-\boldsymbol{n}^-, \qquad \forall \text{ scalar-valued functions } v.$$

$$\{\!\{\boldsymbol{\tau}\}\!\} = \frac{\boldsymbol{\tau}^+ + \boldsymbol{\tau}^-}{2}, \quad [\![\boldsymbol{\tau}]\!] = \boldsymbol{\tau}^+\cdot\boldsymbol{n}^+ + \boldsymbol{\tau}^-\cdot\boldsymbol{n}^-, \quad \forall \text{ vector-valued functions } \boldsymbol{\tau}.$$

$$\{\!\{v\}\!\} = \frac{v^+ + v^-}{2}, \quad [\![v]\!] = v^+\boldsymbol{n}^+ + v^-\boldsymbol{n}^-, \qquad \forall \text{ scalar-valued functions } v.$$

$$\{\!\{\boldsymbol{\tau}\}\!\} = \frac{\boldsymbol{\tau}^+ + \boldsymbol{\tau}^-}{2}, \quad [\![\boldsymbol{\tau}]\!] = \boldsymbol{\tau}^+\cdot\boldsymbol{n}^+ + \boldsymbol{\tau}^-\cdot\boldsymbol{n}^-, \quad \forall \text{ vector-valued functions } \boldsymbol{\tau}.$$

Numerical Fluxes

$$ik\widehat{\boldsymbol{\sigma}}_{hp} = \begin{cases} \{\!\{\nabla_h u_{hp}\}\!\} - \alpha ik[\![u_{hp}]\!] & \text{on interior faces,} \\ \nabla_h u_{hp} - (1-\delta)\left(\nabla_h u_{hp} + ik\vartheta u_{hp}\boldsymbol{n} - g_R\boldsymbol{n}\right) & \text{on faces on } \Gamma_R, \\ 0 & \text{on faces on } \Gamma_N, \\ \nabla_h u_{hp} - \alpha ik u_{hp}\boldsymbol{n} & \text{on faces on } \Gamma_D, \end{cases}$$

$$\widehat{u}_{hp} = \begin{cases} \{\!\{u_{hp}\}\!\} - \beta(ik)^{-1}[\![\nabla_h u_{hp}]\!] & \text{on interior faces,} \\ u_{hp} - \delta\left((ik\vartheta)^{-1}\nabla_h u_{hp}\cdot\boldsymbol{n} + u_{hp} - (ik\vartheta)^{-1}g_R\right) & \text{on faces on } \Gamma_R, \\ u_{hp} - \beta(ik)^{-1}\nabla_h u_{hp}\cdot\boldsymbol{n} & \text{on faces on } \Gamma_N, \\ 0 & \text{on faces on } \Gamma_D, \end{cases}$$

with flux parameters α, β, $0 < \delta \leq 1/2$.

Trefftz Discontinuous Galerkin FEM for Helmholtz

Find $u_{hp} \in V_p(\mathcal{T}_h)$ such that,

$$\mathcal{A}_h(u_{hp}, v_{hp}) = \ell_h(v_{hp}),$$

for all $v_{hp} \in V_p(\mathcal{T}_h)$, where

$$\begin{aligned}
\mathcal{A}_h(u,v) = &\int_{\mathcal{F}_h^I \cup \mathcal{F}_h^N} \{\!\{u\}\!\} [\![\nabla_h \bar{v}]\!] \, ds - \int_{\mathcal{F}_h^I \cup \mathcal{F}_h^N} \beta (ik)^{-1} [\![\nabla_h u]\!][\![\nabla_h \bar{v}]\!] \, ds \\
&- \int_{\mathcal{F}_h^I \cup \mathcal{F}_h^D} \{\!\{\nabla_h u\}\!\} \cdot [\![\bar{v}]\!] \, ds + \int_{\mathcal{F}_h^I \cup \mathcal{F}_h^D} \alpha ik [\![u]\!] \cdot [\![\bar{v}]\!] \, ds \\
&+ \int_{\mathcal{F}_h^R} (1-\delta) u \nabla_h \bar{v} \cdot \boldsymbol{n} \, ds - \int_{\mathcal{F}_h^R} \delta (ik\vartheta)^{-1} (\nabla_h u \cdot \boldsymbol{n})(\nabla_h \bar{v} \cdot \boldsymbol{n}) \, ds \\
&- \int_{\mathcal{F}_h^R} \delta \nabla_h u \cdot \boldsymbol{n} \bar{v} \, ds + \int_{\mathcal{F}_h^R} (1-\delta) ik\vartheta u \bar{v} \, ds, \\
\ell_h(v) = &- \int_{\mathcal{F}_h^R} \delta (ik\vartheta)^{-1} g_R \nabla_h \bar{v} \cdot \boldsymbol{n} \, ds + \int_{\mathcal{F}_h^R} (1-\delta) g_R \bar{v} \, ds.
\end{aligned}$$

Penalty Type	α	β	δ
DG-type Gittelson, Hiptmair & Perugia, 2009	$\mathtt{a}q_K^2/kh_K$	$\mathtt{b}kh_K/q_K$	$\mathtt{d}kh_K/q_K$
Constant Hiptmair, Moiola & Perugia, 2011	$\mathtt{a}$	$\mathtt{b}$	$\mathtt{d}$
UWVF Cessenat & Després, 1998	$1/2$	$1/2$	$1/2$
Non-Uniform Mesh Hiptmair, Moiola & Perugia, 2014	$\mathtt{a}h_{\mathsf{max}}/h_K$	$\mathtt{b}h_{\mathsf{max}}/h_K$	$\mathtt{d}h_{\mathsf{max}}/h_K$

For the rest of this talk we ignore Neumann boundary conditions.

Flux Parameters

Penalty Type	α	β	δ
DG-type Gittelson, Hiptmair & Perugia, 2009	$\mathtt{a} q_K^2 / k h_K$	$\mathtt{b} k h_K / q_K$	$\mathtt{d} k h_K / q_K$
Constant Hiptmair, Moiola & Perugia, 2011	$\mathtt{a}$	$\mathtt{b}$	$\mathtt{d}$
UWVF Cessenat & Després, 1998	$1/2$	$1/2$	$1/2$
Non-Uniform Mesh Hiptmair, Moiola & Perugia, 2014	$\mathtt{a} h_{\max} / h_K$	$\mathtt{b} h_{\max} / h_K$	$\mathtt{d} h_{\max} / h_K$

For the rest of this talk we ignore Neumann boundary conditions.

Energy Norm

$$\|v\|_{\mathrm{TDG}}^2 = k \left\| \alpha^{1/2} [\![v]\!] \right\|_{L^2(\mathcal{F}_h^I \cup \mathcal{F}_h^D)}^2 + \frac{1}{k} \left\| \beta^{\frac{1}{2}} [\![\nabla v]\!] \right\|_{L^2(\mathcal{F}_h^I)}^2 + \frac{1}{k\vartheta} \left\| \delta^{1/2} \nabla v \cdot \boldsymbol{n}_K \right\|_{L^2(\mathcal{F}_h^R)}^2 + k\vartheta \left\| (1-\delta)^{1/2} v \right\|_{L^2(\mathcal{F}_h^R)}^2$$

Define the weighted Sobolev norm

$$\|v\|_{H^s(\Omega),k} = \sum_{j=0}^{s} k^{2(s-j)} |v|^2_{H^j(\Omega)}.$$

Define the weighted Sobolev norm

$$\|v\|_{H^s(\Omega),k} = \sum_{j=0}^{s} k^{2(s-j)} |v|^2_{H^j(\Omega)}.$$

Theorem (*a priori* — Non-Uniform Mesh & Non-Uniform Parameters)

Let u be the analytical solution with $u|_K \in H^{s_K+1}(K)$, u_{hp} the TDG solution. For sufficiently large q_K (and assuming $q_K > 2s_K + 1$)

$$\|u - u_p\|_{L^2(\Omega)} \leq C d_\Omega^2 [(d_\Omega k)^{-1} + (d_\Omega^{-1} h)^{s_K + 1/2}] \times \sum_{K \in \mathcal{T}_h} C_K h_K^{s_K - 1} \left(\frac{1}{\widehat{q}_K}\right)^{s_K - 1/2} \|u\|_{H^{s+1}(\Omega),k},$$

where C_K depends on kh_K (as an increasing function) and s_K. Here, $\widehat{q}_K = q_K / \log(q_k+2)$. [Hiptmair, Moiola & Perugia, 2014]

Comparison of Flux Parameters (2D)

Consider the smooth (analytic) solution (for Acoustic Wave Propagation)

$$u(r, \theta) = \mathcal{J}_1(kr)\cos(\theta)$$

on the domain $\Omega = (0, 1) \times (-1/2, 1/2)$.

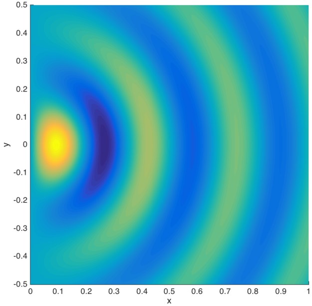

Re(Anal. Soln.) (k=20)

Comparison of Flux Parameters (2D)

Consider the smooth (analytic) solution (for Acoustic Wave Propagation)

$$u(r,\theta) = \mathcal{J}_1(kr)\cos(\theta)$$

on the domain $\Omega = (0,1) \times (-1/2, 1/2)$.
We solve using constant (solid line) and DG-type parameters (dashed).

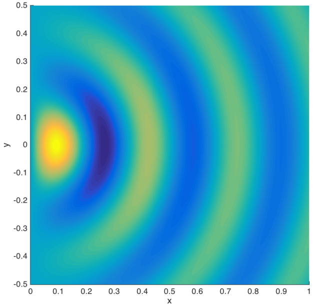

Re(Anal. Soln.) (k=20)

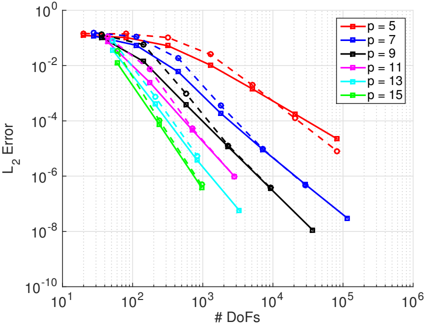

$k = 20$

Consider the smooth (analytic) solution (for Acoustic Wave Propagation)

$$u(r,\theta) = \mathcal{J}_1(kr)\cos(\theta)$$

on the domain $\Omega = (0,1) \times (-1/2, 1/2)$.
We solve using constant (solid line) and DG-type parameters (dashed).

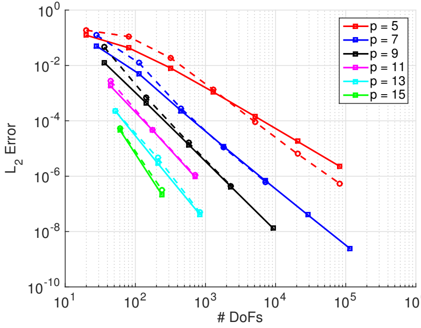

$k = 10$

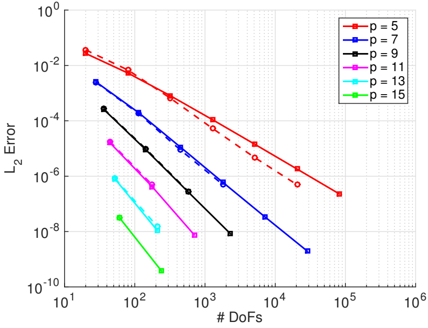

$k = 5$

Comparison of Flux Parameters (3D)

Consider the smooth (analytic) solution (for Acoustic Wave Propagation)

$$u(\boldsymbol{x}) = \mathrm{e}^{ik\boldsymbol{d}\cdot\boldsymbol{x}}$$

on the domain $\Omega = (0,1)^3$, with $k = 20$ and $\boldsymbol{d} = (1/\sqrt{3}, 1/\sqrt{3}, 1/\sqrt{3})$.

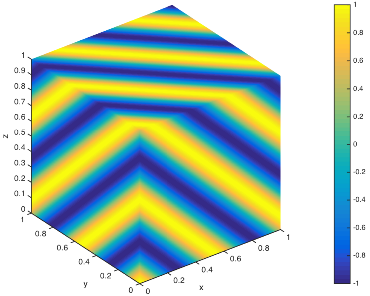

Re(Anal. Soln.)

Comparison of Flux Parameters (3D)

Consider the smooth (analytic) solution (for Acoustic Wave Propagation)

$$u(\boldsymbol{x}) = \mathrm{e}^{ik\boldsymbol{d}\cdot\boldsymbol{x}}$$

on the domain $\Omega = (0,1)^3$, with $k = 20$ and $\boldsymbol{d} = (1/\sqrt{3}, 1/\sqrt{3}, 1/\sqrt{3})$.
We solve using constant (solid line) and DG-type parameters (dashed).

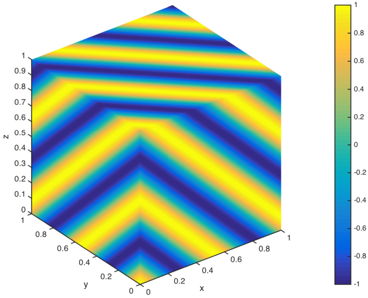

Re(Anal. Soln.)

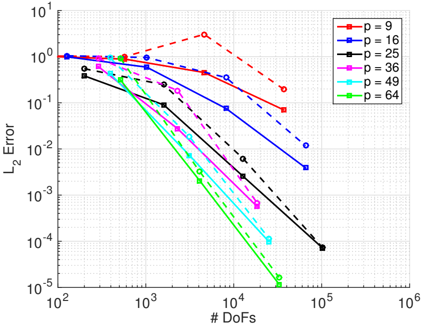

$\|u - u_{hp}\|_{L^2(\Omega)}$ vs. Degrees of Freedom

To test the non-uniform parameters, we consider the solution

$$u(x,y) = \mathcal{H}_0^{(1)}(k\sqrt{x^2+y^2}),$$

with $k = 50$, on the domain $\Omega = (0,1)^2$, where $\mathcal{H}_0^{(1)}$ represents the Hankel function of the first kind of order 0.

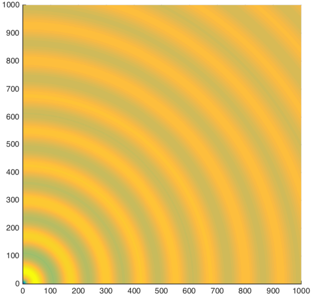

Im(Anal. Soln.)

To test the non-uniform parameters, we consider the solution

$$u(x, y) = \mathcal{H}_0^{(1)}(k\sqrt{x^2 + y^2}),$$

with $k = 50$, on the domain $\Omega = (0, 1)^2$, where $\mathcal{H}_0^{(1)}$ represents the Hankel function of the first kind of order 0.

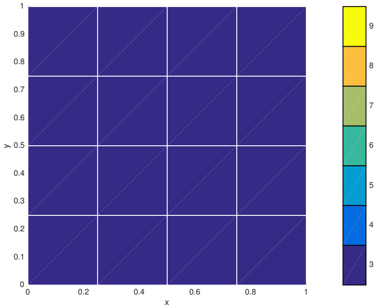

Mesh 1

To test the non-uniform parameters, we consider the solution

$$u(x,y) = \mathcal{H}_0^{(1)}(k\sqrt{x^2+y^2}),$$

with $k = 50$, on the domain $\Omega = (0,1)^2$, where $\mathcal{H}_0^{(1)}$ represents the Hankel function of the first kind of order 0.

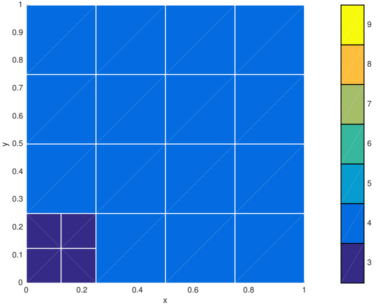

Mesh 2

Comparison of Flux Parameters (Non-Unif.)

To test the non-uniform parameters, we consider the solution

$$u(x, y) = \mathcal{H}_0^{(1)}(k\sqrt{x^2 + y^2}),$$

with $k = 50$, on the domain $\Omega = (0, 1)^2$, where $\mathcal{H}_0^{(1)}$ represents the Hankel function of the first kind of order 0.

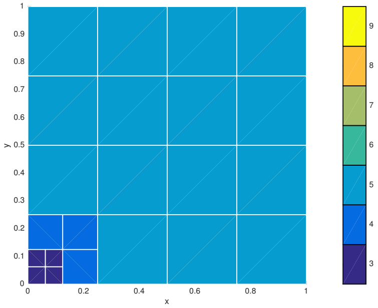

Mesh 3

To test the non-uniform parameters, we consider the solution

$$u(x, y) = \mathcal{H}_0^{(1)}(k\sqrt{x^2 + y^2}),$$

with $k = 50$, on the domain $\Omega = (0, 1)^2$, where $\mathcal{H}_0^{(1)}$ represents the Hankel function of the first kind of order 0.

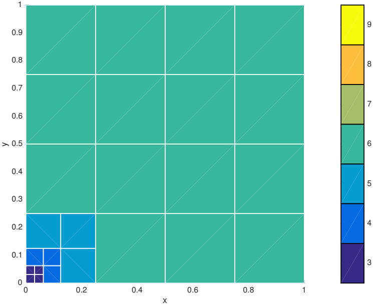

Mesh 4

To test the non-uniform parameters, we consider the solution

$$u(x, y) = \mathcal{H}_0^{(1)}(k\sqrt{x^2 + y^2}),$$

with $k = 50$, on the domain $\Omega = (0, 1)^2$, where $\mathcal{H}_0^{(1)}$ represents the Hankel function of the first kind of order 0.

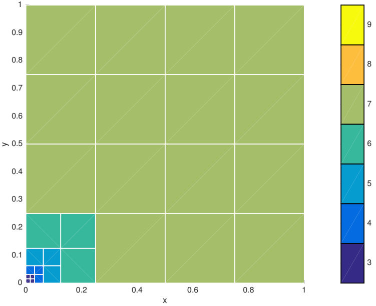

Mesh 5

To test the non-uniform parameters, we consider the solution

$$u(x, y) = \mathcal{H}_0^{(1)}(k\sqrt{x^2 + y^2}),$$

with $k = 50$, on the domain $\Omega = (0, 1)^2$, where $\mathcal{H}_0^{(1)}$ represents the Hankel function of the first kind of order 0.

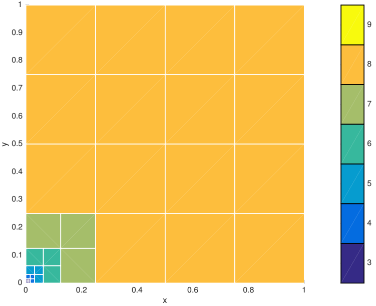

Mesh 6

Comparison of Flux Parameters (Non-Unif.)

To test the non-uniform parameters, we consider the solution

$$u(x,y) = \mathcal{H}_0^{(1)}(k\sqrt{x^2+y^2}),$$

with $k = 50$, on the domain $\Omega = (0,1)^2$, where $\mathcal{H}_0^{(1)}$ represents the Hankel function of the first kind of order 0.

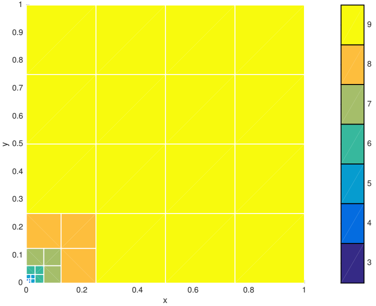

Mesh 7

Comparison of Flux Parameters (Non-Unif.)

To test the non-uniform parameters, we consider the solution

$$u(x,y) = \mathcal{H}_0^{(1)}(k\sqrt{x^2+y^2}),$$

with $k = 50$, on the domain $\Omega = (0,1)^2$, where $\mathcal{H}_0^{(1)}$ represents the Hankel function of the first kind of order 0.

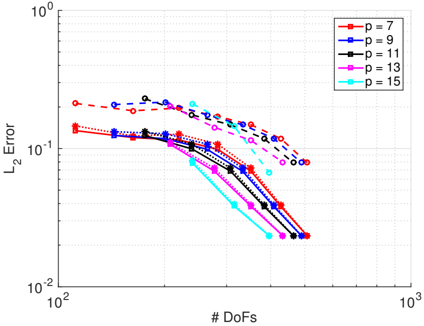

Constant (solid line), DG-type (dashed) & non-uniform (dotted) parameters

Non-Uniform Flux Parameters

The non-uniform mesh parameter has one issue.

Non-Uniform Flux Parameters

The non-uniform mesh parameter has one issue.

We require that

$$\delta = \mathtt{d}\frac{h_{\max}}{h_K} \leq \frac{1}{2} \qquad \Longrightarrow \qquad \mathtt{d} \leq \frac{h_K}{2h_{\max}} \text{ for all } K \in \mathcal{T}.$$

Non-Uniform Flux Parameters

The non-uniform mesh parameter has one issue.

We require that

$$\delta = \mathtt{d}\frac{h_{\max}}{h_K} \leq \frac{1}{2} \qquad \Longrightarrow \qquad \mathtt{d} \leq \frac{h_K}{2h_{\max}} \text{ for all } K \in \mathcal{T}.$$

The smallest value of this ration occurs when $h_K = h_{\min}$; hence,

$$\mathtt{d} \leq \frac{h_{\min}}{2h_{\max}}$$

and $\mathtt{d}$ is, therefore, dependent on the ratio between the largest and smallest element in the mesh.

A posteriori Error Estimates

Ignoring Neumann boundary conditions *a posteriori* error bounds exists for the h-version of the method in $\mathbb{R}^2$.

Ignoring Neumann boundary conditions *a posteriori* error bounds exists for the *h*-version of the method in $\mathbb{R}^2$.

A posteriori Error Bound — *h*-version Only

For the TDGFEM, with the non-uniform flux parameters, the following error bound holds:

$$\|u - u_{hp}\|_{L^2(\Omega)} \leq C \Big\{ \Big\| \alpha^{1/2} h_F^s [\![u_h]\!] \Big\|_{L^2(\mathcal{F}_h^I \cup \mathcal{F}_h^D)} + \frac{1}{k} \| \beta^{\frac{1}{2}} h_F^s [\![\nabla u_h]\!] \|_{L^2(\mathcal{F}_h^I)} + \frac{1}{k} \Big\| \delta^{1/2} h_F^s \left(g_R - \nabla u_h \cdot \boldsymbol{n}_K + ik\vartheta u_h \right) \Big\|_{L^2(\mathcal{F}_h^R)} \Big\}$$

where s depends on the regularity of the solution to the adjoint problem ($z \in H^{3/2+s}(\Omega)$).

[Kapita, Monk, Warburton (2014 - Tech. Report)]

Consider again the solution

$$u(x, y) = H_0^{(1)}(k(x^2 + y^2)),$$

with $k = 50$, on the domain $\Omega = (0, 1)^2$.
We solve using constant (solid line), DG-type (dashed) and non-uniform parameter (dotted).

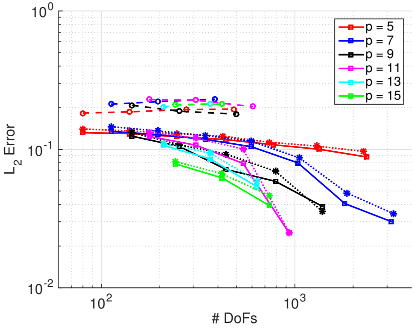

L_2 Error

Consider again the solution

$$u(x,y) = H_0^{(1)}(k(x^2+y^2)),$$

with $k = 50$, on the domain $\Omega = (0,1)^2$.
We solve using constant (solid line), DG-type (dashed) and non-uniform parameter (dotted).

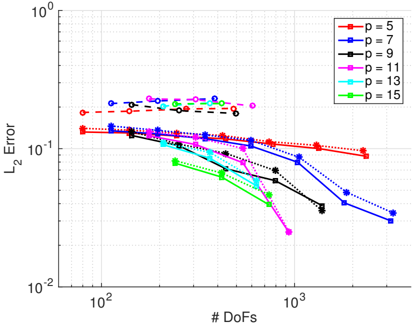

L_2 Error

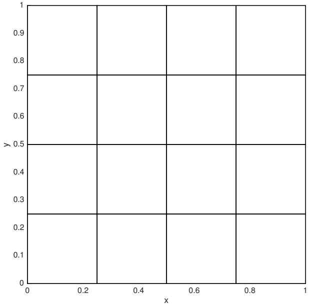

Mesh 1 ($p = 7$)

Consider again the solution

$$u(x,y) = H_0^{(1)}(k(x^2+y^2)),$$

with $k = 50$, on the domain $\Omega = (0,1)^2$.
We solve using constant (solid line), DG-type (dashed) and non-uniform parameter (dotted).

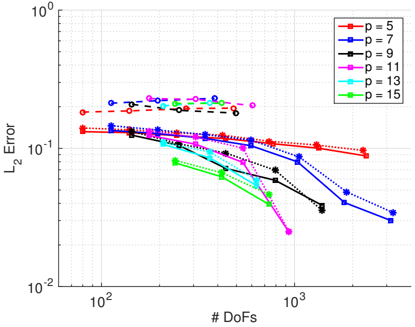

L_2 Error

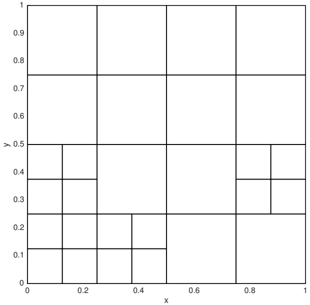

Mesh 2 ($p = 7$)

Consider again the solution

$$u(x,y) = H_0^{(1)}(k(x^2+y^2)),$$

with $k = 50$, on the domain $\Omega = (0,1)^2$.
We solve using constant (solid line), DG-type (dashed) and non-uniform parameter (dotted).

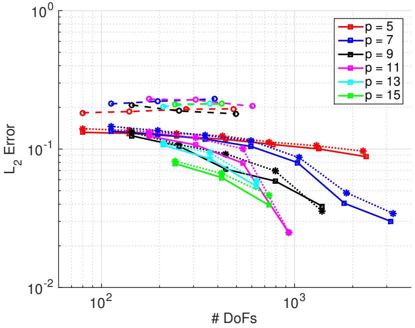

L_2 Error

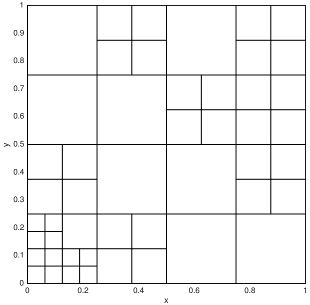

Mesh 3 ($p = 7$)

Consider again the solution

$$u(x,y) = H_0^{(1)}(k(x^2+y^2)),$$

with $k = 50$, on the domain $\Omega = (0,1)^2$.
We solve using constant (solid line), DG-type (dashed) and non-uniform parameter (dotted).

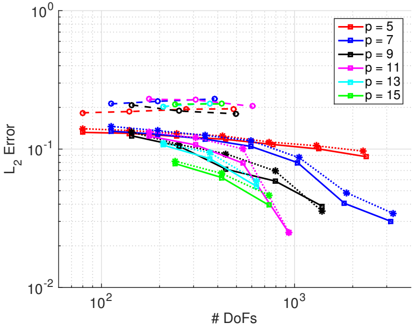

L_2 Error

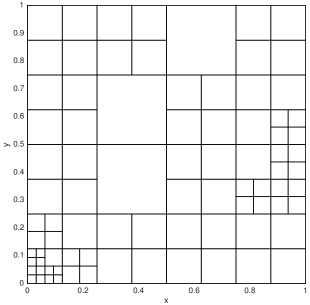

Mesh 4 ($p = 7$)

Consider again the solution

$$u(x,y) = H_0^{(1)}(k(x^2+y^2)),$$

with $k = 50$, on the domain $\Omega = (0,1)^2$.
We solve using constant (solid line), DG-type (dashed) and non-uniform parameter (dotted).

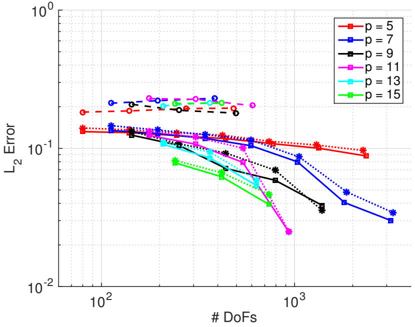

L_2 Error

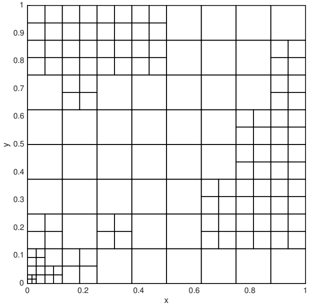

Mesh 5 ($p = 7$)

Consider again the solution

$$u(x,y) = H_0^{(1)}(k(x^2 + y^2)),$$

with $k = 50$, on the domain $\Omega = (0,1)^2$.
We solve using constant (solid line), DG-type (dashed) and non-uniform parameter (dotted).

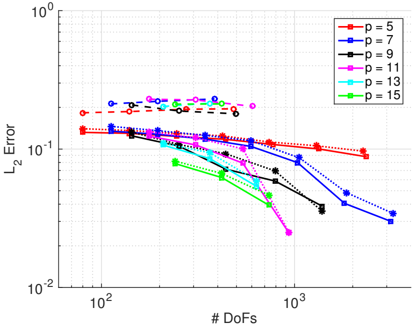

L_2 Error

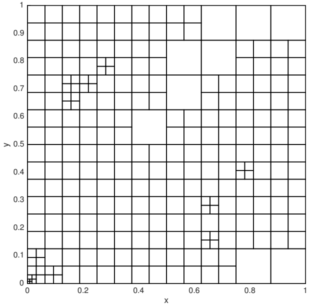

Mesh 6 ($p = 7$)

Conclusion

Summary:

- *A priori* error results exist for Trefftz DG, with Robin and Dirichlet boundary conditions

Conclusion

Summary:

- *A priori* error results exist for Trefftz DG, with Robin and Dirichlet boundary conditions
- The various choice of flux parameters is required for the existing analysis

Conclusion

Summary:

- *A priori* error results exist for Trefftz DG, with Robin and Dirichlet boundary conditions
- The various choice of flux parameters is required for the existing analysis
- The choice of flux parameters tends to make no difference on smooth solutions, although DG-style parameters appear poor for non-uniform refinement/singular problems.

Summary:

- *A priori* error results exist for Trefftz DG, with Robin and Dirichlet boundary conditions
- The various choice of flux parameters is required for the existing analysis
- The choice of flux parameters tends to make no difference on smooth solutions, although DG-style parameters appear poor for non-uniform refinement/singular problems.

Future Aims:

Conclusion

Summary:

- *A priori* error results exist for Trefftz DG, with Robin and Dirichlet boundary conditions
- The various choice of flux parameters is required for the existing analysis
- The choice of flux parameters tends to make no difference on smooth solutions, although DG-style parameters appear poor for non-uniform refinement/singular problems.

Future Aims:

- Extend the existing *a posteriori* error analysis to *hp*-version meshes (ideally for constant flux parameters).

Conclusion

Summary:

- *A priori* error results exist for Trefftz DG, with Robin and Dirichlet boundary conditions
- The various choice of flux parameters is required for the existing analysis
- The choice of flux parameters tends to make no difference on smooth solutions, although DG-style parameters appear poor for non-uniform refinement/singular problems.

Future Aims:

- Extend the existing *a posteriori* error analysis to *hp*-version meshes (ideally for constant flux parameters).
- Develop an algorithm for deciding on whether to perform h or p refinement.

Conclusion

Summary:

- *A priori* error results exist for Trefftz DG, with Robin and Dirichlet boundary conditions
- The various choice of flux parameters is required for the existing analysis
- The choice of flux parameters tends to make no difference on smooth solutions, although DG-style parameters appear poor for non-uniform refinement/singular problems.

Future Aims:

- Extend the existing *a posteriori* error analysis to *hp*-version meshes (ideally for constant flux parameters).
- Develop an algorithm for deciding on whether to perform *h* or *p* refinement.
- Analysis for Neumann boundary conditions (missing required fundamental result - stability of solution on the continuous level).